Ultrasonics Sonochemistry 89 (2022) 106108

Contents lists available at ScienceDirect

Ultrasonics Sonochemistry

journal homepage: www.elsevier.com/locate/ultson

Ultrasonic-assisted pH shift-induced interfacial remodeling for enhancing the emulsifying and foaming properties of perilla protein isolate

Jing Yang [a,b], Yuqing Duan [b,c], Fang Geng [d], Chen Cheng [a], Lei Wang [a], Jieting Ye [a], Haihui Zhang [b], Dengfeng Peng [a,*], Qianchun Deng [a,*]

[a] Oil Crops Research Institute, Chinese Academy of Agricultural Sciences, Key Laboratory of Oilseeds Processing, Key Laboratory of Oilseeds Processing, Ministry of Agriculture and Rural Affairs, Oil Crops and Lipids Process Technology National & Local Joint Engineering Laboratory, and Hubei Research Center of Oil and Plant Protein Engineering Technology, Wuhan 430062, Hubei, China
[b] School of Food and Biological Engineering, Jiangsu University, Zhenjiang 212013, China
[c] Institute of Food Physical Processing, Jiangsu University, Zhenjiang 212013, China
[d] Key Laboratory of Coarse Cereal Processing (Ministry of Agriculture and Rural Affairs), School of Food and Biological Engineering, Chengdu University, Chengdu 610106, Sichuan, China

ARTICLE INFO

Keywords:
Ultrasound
Plant protein
Interfacial properties
pH shift
Structure
Functionality

ABSTRACT

In order to expand the applications of plant protein in food formulations, enhancement of its functionalities is meaningful. Herein, the effects of ultrasonic (20 KHz, 400 W, 20 min)-assisted pH shift (pH 10 and 12) treatment on the structure, interfacial behaviors, as well as the emulsifying and foaming properties of perilla protein isolate (PPI) were investigated. Results showed that the solubility of PPI treated by ultrasonic-assisted pH shift (named UPPI-10/12) exceeded 90 %, which was at least 2 and 1.4 times that of untreated PPI and ultrasound-based PPI. Meanwhile, UPPI-10/12 possessed higher foamability (increasing by at least 1.2 times) and good emulsifying stability. Ultrasonic-assisted pH shift treatment decomposed large PPI aggregates into tiny particles, evident from the dynamic light scattering (DLS) and atomic force microscopy results. Besides, this approach induced a decrease in α-helix of PPI and an increase in β-sheet, which might result in the exposure of the hydrophobic group on the structural surface of PPI, thus leading to the increase of surface hydrophobicity. The smaller size and higher hydrophobicity endowed UPPI-10/12 faster adsorption rate, tighter interfacial structure, and higher elastic modulus at the air- and oil–water interfaces, evident from the cryo-SEM and interfacial dilatational rheological results. Thus, the emulsifying and foaming properties could evidently enhance. This study demonstrated that ultrasonic-assisted pH shift technique was a simple approach to effectively improve the functional performance of PPI.

1. Introduction

The population growth and global consumption pattern change towards higher protein-based food intake have aroused people's concerns about the shortage of protein resources [1]. This prompts researchers to conduct extensive studies to find new and sustainable protein sources. In order to alleviate the impact on the environment and climate change, plant proteins are gradually used in food processing due to their advantages, such as larger yield, fewer carbon emissions, and more health [2]. Perilla, which belongs to the *Lamiaceae* family, is introduced to Europe as an oil crop. It is widely utilized as a medicinal material and food ingredient. Perilla seeds are rich in oil (39 %–58 %) and protein (20 %–30 %), similar to soy and peanut. After oil processing, a large amount of perilla meal is produced, which is mainly used as agricultural fertilizer or animal feed. This leads to the waste of beneficial ingredients. Perilla meal is rich in protein (35 %–45 %), which contains all kinds of essential amino acids and possesses a relatively reasonable amino acid composition. Studies showed that perilla protein isolate (PPI) extracted from perilla meals had high nutritional value and prosperous protein efficiency, which could be acted as a new alternative source of animal proteins [3]. Therefore, it is necessary to vigorously develop and utilize PPI to increase the added value of perilla and expand its applications in the food industry [4,5].

Most plant-based proteins display relatively poor functionalities

* Corresponding authors.
E-mail addresses: dfpengfood@outlook.com (D. Peng), dengqianchun@caas.cn (Q. Deng).

https://doi.org/10.1016/j.ultsonch.2022.106108
Received 19 May 2022; Received in revised form 6 July 2022; Accepted 28 July 2022
Available online 30 July 2022

compared to animal proteins, which significantly limits their application value in food formulations. Ultrasound, a green and effective non-thermal modification technology, has broad prospects in the food industry, resulting from its high safety and no chemical reagent residues. Ultrasonic treatment can improve the solubility, surface activity, emulsification, and foaming properties of plant proteins by changing their structural properties and aggregation behaviors, mainly through cavitation effect, mechanical effect, and thermal effect [6-8]. Zhao et al. [9] reported that ultrasonication could reduce the particle size, induce the exposure of its hydrophobic groups, and change the conformation of PPI. This gave it the ability to prepare highly stable emulsions. However, ultrasonic treatment alone has a limited effect on enhancing the functional properties of PPI, which may be due to its compact structure and the formation of considerable aggregates. In order to efficiently improve the functionality of PPI, the protein structure first needs to be unfolded or partially unfolded. pH shift exposes protein solutions to alkaline/acidic pH values and then adjusts to neutral conditions. By this approach, the proteins undergo the structural unfolding and refolding process, which leads to the change of structural properties and surface activities of protein [10]. Jiang et al. [11] stated that a protein dominated by globulin might partly unfold under extreme pH shift, increasing its flexibility and forming a 'molten globule' structure. This gave it a faster adsorption rate and higher functional properties [12,13]. To achieve synergistic effects, the combination of ultrasound and pH shift has been suggested to greatly improve the available properties of proteins. Lee et al. [14] showed that ultrasonic-assisted pH 12 shift treatment could reduce the size and increase the surface hydrophobicity of soluble soybean protein aggregates, leading to the enhancement of protein solubility and emulsifying properties. Jiang et al. [15] studied the effect of the ultrasonic-assisted pH shift process on pea protein isolate's structure and functional properties. The particle size was decreased to 45.2 nm, and the surface hydrophobicity significantly improved due to the disruption of disulfide bonds and the exposure of internal hydrophobic residues. Besides, Li et al. [16] discovered that the treatment of rapeseed protein isolate by ultrasonic-assisted pH 12.5 treatment could reduce the particle size (from 330.90 to 115.77 nm) and increase the free sulfhydryl group (11.63 to 24.50 μmol/g) and H_0 (from 2053.9 to 2649.4). These properties provided high solubility (from 8.90 % to 66.84 %) for rapeseed protein. Similar results were also reported modifying rice protein and barley protein by this combined method [2,17]. However, the current research on ultrasonic-assisted pH shift-induced plant protein modification mainly focuses on enhancing functionalities and insight into protein structure. Few studies systematically explore the improvement mechanism of functional characteristics from the interfacial perspective.

In this work, the effects of ultrasonic-assisted pH shift on the structure, interfacial behaviors, and emulsifying and foaming properties of perilla protein isolate were studied. The secondary structure, tertiary structure, surface hydrophobicity (H_0), sodium dodecyl sulfate–polyacrylamide gel electrophoresis (SDS-PAGE), particle size, and zeta potential were measured to characterize the structural properties of PPI. The interfacial rheology, Confocal-Raman microscopy, and cryo-scanning electron microscopy (*cryo*-SEM) captured the interfacial information. The properties of the solubility, emulsifying, and foaming were used to describe protein functional properties. In addition, the relationship among these three behaviors was investigated to understand further the enhancement mechanisms of the emulsifying and foaming properties of PPI. This work provides new strategies for promoting the widespread use of PPI as an active stabilizer in food systems.

2. Materials and methods

2.1. Materials

Perilla seed was supplied by the Tongrentang (Bozhou, Anhui, China). 8-Anilino-1-naphthalene sulfonic acid (ANS) (St. Louis, Missouri, USA). All other reagents used were of analytical grade.

2.2. Preparation of PPI

The PPI was extracted by the alkali-dissolved acid precipitation method. First, the defatted perilla powders were got by cold pressing (CA59G cold press, Komet, Germany) and grinding of perilla seeds. Then, the powders were dissolved in ultrapure water at a ratio of 1:15 (w/v). The supernatant was obtained after stirring the solution by adjusting the pH to 9 at room temperature (25 °C) for 2 h and centrifuging (7000 rpm, 4 °C, 20 min). Subsequently, it was stirred and centrifuged again (7000 rpm, 4 °C, 20 min) after adjusting the pH to 4.5 with 1 M HCl, followed by collecting of the precipitation. The pellet was resuspended in ultrapure water for 2 h by adjusting the pH to 7.0 with 1 M NaOH. After using a freeze-dryer, the PPI powders were obtained. Kjeldahl method [3] was used to determine the protein content, and the result was 87.03 ± 0.11 %.

2.3. Ultrasound and ultrasonic-assisted pH shift treatments

The initial protein concentration of PPI was 10 mg/mL, and then the protein was stirred for 2 h to dissolve fully. The pH was adjusted to 10 and 12 with 1 M NaOH. The protein solution was stirred at 25 °C for 2 h and then subjected to ultrasound treatment by a JY92-IIDN ultrasound device (45 % of 900 W, Frequency 20 kHz, a cycle of pulses of 2 s on and 2 s off, Ningbo Scientz Biotechnology Co., ltd, China) for 20 min [18]. Afterward, all the samples were adjusted to pH 7.0 by adding 1 M HCl. These samples are named UPPI-10 and UPPI-12, respectively. The ultrasound treatment alone was named UPPI. The pH was adjusted to 10 and 12 with 1 M NaOH, and the protein solution was stirred at 25 °C for 2 h, and then the pH was neutralized to pH 7 (called PPI-10 and PPI-12, respectively).

2.4. Circular dichroism

The circular dichroism (CD) scanning range of wavelength was 190–260 nm. The bandwidth and path length were 1.0 nm and 100 mm, respectively (J-1500, JASCO Japan,). The α-helix, β-sheet, β-turn, and random coil were analyzed using the CD Pro software. We use the model of Yang's reference to fit protein secondary structure. [19,20].

2.5. Intrinsic fluorescence

The fluorescence spectrum of tryptophan intrinsic emission of the sample (0.2 mg/mL) was determined by a fluorescence spectrophotometer (F-7000, HITACHI, Japan). The excitation wavelength and scanning range of emission wavelength were 280 nm and 300–500 nm, respectively The width of the excitation slit and emission slit were both 2.5 nm [21].

2.6. Surface hydrophobicity (H_0)

A protein solution of 0.025 to 0.4 mg/mL was prepared by dilution. 20 μL 8.0 mmol/L ANS solution was added to a protein solution of 4.0 mL. Fluorescence intensity at an excitation wavelength of 390 nm and emission wavelength of 410–650 nm were measured by fluorescence spectrophotometer (F-7000, HITACHI, Japan). The curve was drawn with protein concentration as abscise and fluorescence intensity as ordinate. The slope of the curve was the surface hydrophobicity index of the protein [22].

2.7. Reducing and non-reducing sodium dodecyl sulfate–polyacrylamide gel electrophoresis (SDS-PAGE)

PPI solution (2 mg/mL) was mixed with 10 μL sample dissolve buffer (10 % glycerin, 3 % sodium dodecyl sulfate (SDS), 0.05 % bromophenol

blue, and 5 % β-mercaptoethanol) (non-reducing SDS-PAGE did not using β-mercaptoethanol). Then the sample was heated at 100 °C for 5 min. 10 μL of sample was added into the gel pore, and use 12 % separating gel and 5 % stacking gel. Gels were run at 60 V for 30 min and 120 V for 1.5 h prior to staining with Coomassie brilliant blue R-250 solution [23,24].

2.8. Particle size and ζ-potential measurements

The sample concentration was 1 mg/mL in ultrapure water, and the particle size and ζ-potential of the sample were analyzed by Malvern ZetaSizer nano-ZS laser particle size distribution analyzer (Zetasizer Pro, Malvern Instruments, Worcestershire, UK). [25].

2.9. Atomic force microscopy (AFM) analysis

5 μL of protein sample (10 μg/mL) was deposited in a mica plate and wait to dry. The images were obtained by using the atomic force microscosy (Bruker Dimension ICON, USA) [26].

2.10. Interfacial adsorption behavior

Interfacial tension of samples at the oil- and air–water interface was measured by a drop profile tensiometer (Tracker, Teclis Technologies, France). MCT was used as the oil phase and the aqueous phase was different protein samples (0.2 mg/mL) [27]. Each experiment was monitored for 3600 s at 25 ℃. The droplet area was maintained at volume 6.5 mm^3. The values of the surface tension (γ) were calculated by analyzing the shape of the pendent drop according to the Young-Laplace equation (1)[28].

$$\Delta P = \gamma\left(\frac{1}{R_1}+\frac{1}{R_2}\right) \tag{1}$$

where ΔP is Laplace pressure (the pressure difference across fluid interface), R_1 and R_2 are the orthogonal maximum curvature radii of the elongated drop. The drop profiles were continuously monitored, hence the reduction in γ could be recorded as a function of time.

2.11. Interfacial dilatational rheology

Sinusoidal interfacial compression and expansion were performed through changing the droplet area at 10 % of deformation amplitude and 0.1 Hz of angular frequency. The bubble was analyzed to repeated measurements of 4 sinusoidal oscillation cycles and 4 static oscillation cycles for up to 40 min. The surface viscoelastic modulus (E), elastic modulus (E_d), and viscous modulus (E_v) components were derived from the change in surface tension (γ) (dilatational stress). Details of this experiment were described elsewhere [25,29].

2.12. Interfacial morphology of emulsions captured by cryo-SEM

The interfacial microstructure of emulsions stabilized by samples was analyzed by cryo-scanning electron microscopy (cryo-SEM) (SU8010, Hitachi, Japan). The emulsions (5.0–10.0 μL) were frozen in liquid nitrogen and transferred into a cryo-preparation chamber. Then it was cut into the cross-section and sublimated at −90 °C. Following the sputter-coating for 30 s at 5 mA, the interfacial morphology of emulsion droplets and continuous bulk phase were observed using cryo-SEM [30].

2.13. Interfacial structure of PPI measured by Confocal-Raman microscopy

The Raman spectra of PPI adsorbed at the MCT-water interface was obtained using a RENISHAW Raman spectrometer (Gloucestershire GL 12 8JR, UK). The measurement position of the emulsion stabilized by PPI was shown in the Supporting Information. The spectra of the samples, MCT, and PPI at bulk solution were collected at 633 m, and the time was set at 10 s. The Raman spectra were scanned in the regions of 600–1800 cm^{-1} [31].

2.14. Solubility

The samples were diluted with ultrapure water to prepare 1 mg/mL solution. After the centrifugation (4000 r/min, 10 min, 4 ℃), the supernatants were gathered. The protein concentration was measured through the Bradford method using BSA as the standard protein [32]. The following equation (2) was used to determine the protein solubility (%):

$$Solubility\ (\%) = \frac{Protein\ content\ of\ supernatant\ \times 100}{Total\ protein\ content\ of\ sample\ before\ centrifugation} \tag{2}$$

2.15. Emulsifying properties

The emulsifying activity index (EAI) and emulsification stability (ESI) were used as indexes. Differently treated 1 % PPI solutions were prepared. The 15 mL treated samples were mixed with 5 mL MCT oil for homogenate (IKA, T25, Germany) at 13000 rpm for 2 min. The freshly prepared emulsion (50 μL) was mixed with 5 mL 0.1 % SDS, and measured absorbance at 500 nm (A_0). The emulsion was stored at room temperature for 10 min and the light absorption was measured again (A_{10}) [33]. EAI and ESI are calculated by the following formula (3) and (4):

$$EAI\ (m^2/g) = \frac{2 \times 2.303 \times A_0 \times DF}{\theta \times C \times 10000} \tag{3}$$

$$ESI\left(\ \min\ \right) = \frac{A_0 \times \Delta T}{\Delta A} \times 100\% \tag{4}$$

where DF, C, and θ represent the dilution factor, protein concentration, and oil volume fraction, respectively. ΔA represent the difference between A_0 and A_{10}.

2.16. Foaming properties

Place the fresh sample solution (15 mL) in a glass bottle and use a homogenizer (IKA, T25, Germany) stirring at 13000 rpm for 2 min. After stirring, the foam was immediately poured into a 50 mL measuring cylinder. Foamability (FA) was characterized by comparing the foam volume at 2 min (V_2) with the initial liquid volume of samples (15 mL) [34]. Foam stability (FS) was determined by comparing the foam volume at 60 min with the initial foam volume [35]. FA and FS are calculated by the following formula (5) and (6):

$$FA\ (\%) = \frac{V_2}{15} \times 100 \tag{5}$$

$$FS\ (\%) = \frac{V_{60}}{V_2} \times 100 \tag{6}$$

where V_2 is the foam volume at 2 min and V_{60} is the foam volume at 60 min.

2.17. Statistics analysis

All tests were measured three times. One-way ANOVA was performed by SPSS 26.0 and $p < 0.05$ was considered as the significant level.

3. Results and discussion

3.1. Structural properties of PPI

3.1.1. Circular dichroism

As shown in Fig. 1**A**, CD spectra of all samples have similar shapes, and PPI has an obvious peak around 208 and 222 nm. A positive peak around 190 nm, which is the typical peak of α-helix structure. The β-sheet structure had a negative peak at 210 ~ 225 nm. The percentages of α-helix, β-sheet, β-turn, and random coil of native PPI were 32.05 %, 20.9 %, 16.95 %, and 30.10 %, respectively (Fig. 1**B**). Compared to PPI, the proportion of α-helix of UPPI decreased to 15.80 %, whereas, the β-sheet increased to 43.50 %. The β-turn and random coil decreased slightly. When the PPI was treated by ultrasonic-assisted pH shift treatment, α-helix was further decreased (UPPI-12 was 13.9 %), and β-sheet was significantly increased (UPPI-12 was 50.3 %). These results were consistent with the work reported by Zou et al. [36]. In general, the β-sheet is the most tightly connected structure in a protein molecule. Thus, the increase in the percentage of β-sheet indicated that the protein structure became tighter under ultrasonic-assisted pH shift treatment. It might be due to the strong microfluidic generated by mechanical vibration and cavitation effect, which leads to the collision of protein molecules and the formation of compact structures [37].

3.1.2. Intrinsic fluorescence spectroscopy

Fluorescence spectroscopy is carried out to analyze the changes in the tertiary structure of PPI, and results are exhibited in Fig. 1**C**. The changes in the fluorescence spectroscopy are mainly caused by the presence of tryptophan, phenylalanine, and tyrosine residues [38]. The wavelength of PPI was about 330 nm. The fluorescence intensity of PPI was significantly enhanced after ultrasound treatment ($p < 0.05$). These results were consistent with previous studies [39]. Ultrasound treatment could affect the structure of PPI, and the peak position of PPI gradually shifted to the right and the polarity became more hydrophilic. These results were also similar to those of the studies on watermelon seed protein and potato protein [26,40]. Besides, the fluorescence intensity of natural PPI was the lowest, indicating that most of the tryptophan residues were wrapped in the protein interior. After ultrasonic-assisted pH shift treatment, the relative fluorescence intensity of PPI was increased, which might be due to the changes in PPI conformation and more chromophores exposed to the solvent.

3.1.3. Surface hydrophobicity (H_0)

The surface hydrophobicity of protein refers to the index of the number of hydrophobic groups on the protein surface in contact with the polar water environment and is closely related to the conformation, interfacial properties, and relevant functional performance of protein [41]. Here, the H_0 is captured and shown in Fig. 1**D**. Compared with PPI (630.78), the H_0 of PPI-12 slightly increased ($p < 0.05$). The H_0 of UPPI-12 increased significantly (1038.5) ($p < 0.05$), which was 1.65 times than that of the control. The hydrophobic sites of proteins were enhanced due to the microfluidic and cavitation effects of ultrasound [42]. Compared with PPI-10/PPI-12 treatment, UPPI-10 and UPPI-12 significantly enhanced the H_0 of PPI ($p < 0.05$), which was consistent with a previous study [43]. The increase of H_0 indicated that the hydrophobic portion of the peptide and the non-polar amino acid side chain groups of the amino acid residues were exposed [44]. In the present work, PPI was structurally unfolded under alkaline treatment, which might further dissociate into individual subunits in combination with sonication. This resulted in the exposure of hydrophobic groups and thus increasing the H_0.

3.1.4. SDS-PAGE

Fig. 2 displays the reducing and non-reducing SDS-PAGE of PPI samples. The molecular weight distribution of PPI was wide, ranging from 15 kDa to 55 kDa (Fig. 2**A**). The main bands on reducing conditions

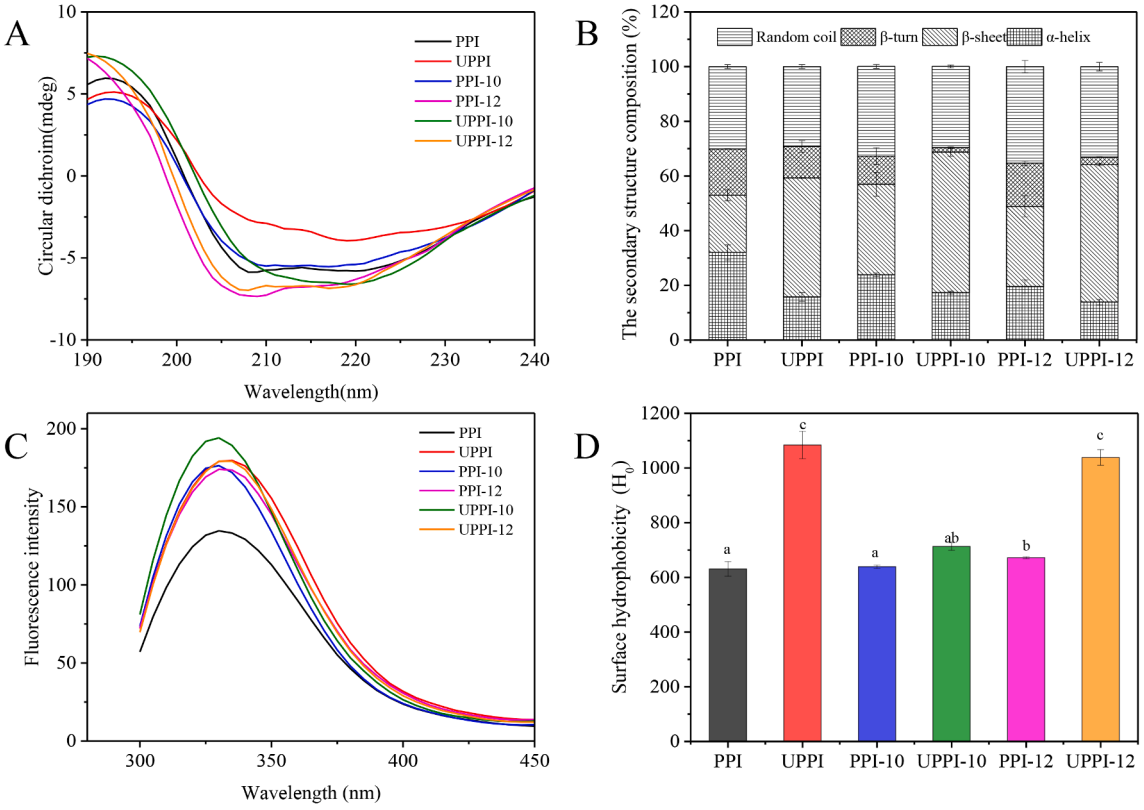

Fig. 1. The circular dichroism (A), secondary structure composition(B), intrinsic fluorescence spectroscopy (C), and surface hydrophobicity (D) of PPI and treated PPI samples.

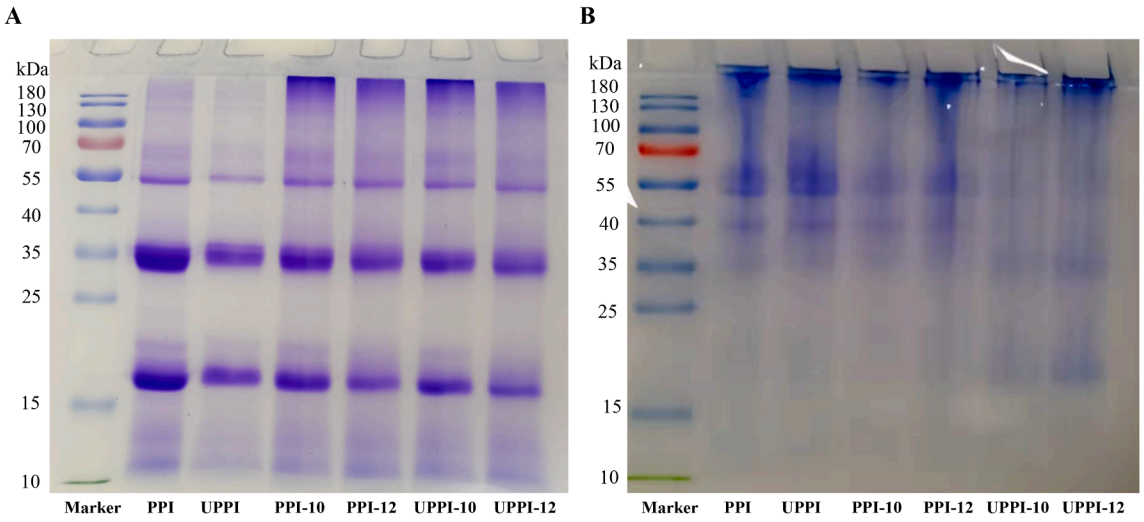

Fig. 2. Sodium dodecylsulfate-polyacrylamide gel electrophoresis (SDS-PAGE) analysis under (A) reducing (with β-mercaptoethanol) and (B) non-reducing conditions of PPI and treated PPI-based samples.

were distributed to ~ 10 kDa, 20 kDa, 35 kDa, and 55 kDa. Compared with the control, the treated PPI samples showed similar electrophoresis spectra, which indicated that ultrasonic-assisted pH shift treatment did not lead to the degradation of the main subunits of PPI into smaller subunits under reducing conditions. The result is consistent with the work reported by Alavi et al. [1]. The non-reducing SDS-PAGE (Fig. 2**B**) image showed that the main bands of PPI were distributed in 40 KDa and 55–70 KDa, which were larger than that of reducing condition. The large molecular weight bands (40–70 KDa) of UPPI-10 and UPPI-12 became weak and appeared at 15–25 KDa. This could be attributed to the cleavage of intermolecular disulfide bonds [14]. The unfolding of the protein structure during pH treatment made the protein more susceptible to sonication [45]. Therefore, the ultrasonic-assisted pH shift treatment could unfold the protein structure and dissociate the large subunits to form small molecular weight subunits.

3.1.5. *Particle size, zeta-potential and atomic force microscopy (AFM) analysis*

Table 1 showed the particle size and zeta potential of investigated PPI-based samples. Except for the UPPI, all treatments reduced the particle size of PPI, especially UPPI-12 had the most obvious effect (71.88 nm), in which the particle size was reduced by 17 times. The particle size of PPI-12 was reduced by 8 times. The particle size of UPPI-10 and UPPI-12 under ultrasonic-assisted pH shift treatment was reduced by about 8 times and 17 times, respectively. Studies showed that ultrasonic treatment at pH 12 could significantly reduce the particle size of soybean protein aggregates, which was similar to our results [14]. The protein structure unfolded during alkaline treatment, and further ultrasound treatment might destroy the hydrogen bond, hydrophobicity, and electrostatic interaction of the protein through the shear force generated by ultrasound cavitation. The partial unfolding of protein structure under alkaline conditions was easier to be modified by ultrasound [46]. Besides, the AFM results of untreated PPI (Fig. 3**A**) showed that the protein dispersibility was poor and the particle size was larger, which was similar to the particle size results. Both PPI-10 and PPI-12 could increase the dispersibility of the protein, and the particle size also decreased to 666.93 nm and 154.13 nm, respectively. The dispersibility of PPI under ultrasonic-assisted pH shift treatment (Fig. 3**E-F**) was further significantly increased, and the particle size of the protein was further reduced to about 100 nm. Similarly, ultrasound can significantly reduce particle size and increase the dispersibility of grape seed protein [47] and watermelon seed protein [26]. Meanwhile, after alkaline shift treatment and ultrasonic-assisted pH shift treatment, the absolute value of the potential value of the protein surface decreased, indicating that the treatment method had the ability to weaken the electrostatic repulsion between protein molecules. The treatment had no obvious effect on the distribution of dissociable amino acid residues on the surface of PPI [1].

3.2. *Interfacial rheological properties*

The dynamic interfacial tension (γ) is a key factor in determining emulsification and foamability [48]. Fig. 4 shows the γ of investigated samples at the oil (MCT)-water **(A-C)** and air–water **(D-F)** interfaces at 25 °C. For the oil–water interface, γ decreased quickly during the initial adsorption period time, showing the adsorption of proteins at the interface. This proved that UPPI-12 had the strongest adsorption capacity at the oil–water interface. UPPI and PPI-10/12 also had the smaller γ when compared with the PPI. This illustrated that both ultrasound alone and pH treatment alone could enhance the adsorption rate of PPI. In the subsequent phases of adsorption, the γ of the UPPI-12 appeared to reach a (nearly) constant value (~7.5 mN/m) for adsorption time larger than 1000 s. Whereas, other samples took a longer time to reach relatively low values (Fig. 4**A-C**). For the air–water interface, γ decreased rapidly during the initial adsorption period, which proved that UPPI-12 had the strongest adsorption capacity at the air–water interface. This indicated that ultrasonic-assisted pH shift treatment can improve the adsorption rate of PPI (Fig. 4**D-F**). The adsorption rate of proteins from the bulk to the oil- and air- water interfaces is relevant to their structural properties, such as particle size, surface hydrophobicity, and zeta potential [49]. In this study, all samples had the similar zeta potential. Compared to other samples, UPPI-12 had a smaller particle size and larger H_0. These allowed it to have a fast diffusion speed and suitable hydrophilic-hydrophobic balance performance, which are the

Table 1
Particle size and ζ-potential of PPI and treated PPI samples.

Samples	PPI	UPPI	PPI-10	UPPI-10	PPI-12	UPPI-12
Particle size (nm)	1218.30 ± 251.31^{c}	1322.67 ± 110.02^{c}	666.93 ± 76.02^{b}	154.13 ± 0.42^{a}	137.07 ± 1.35^{a}	71.88 ± 2.14^{a}
ζ-potential (mV)	-36.23 ± 0.71^{a}	-32.98 ± 1.47^{bc}	-33.47 ± 0.59^{bc}	-33.66 ± 0.78^{b}	-31.60 ± 0.41^{c}	-27.26 ± 1.62^{d}

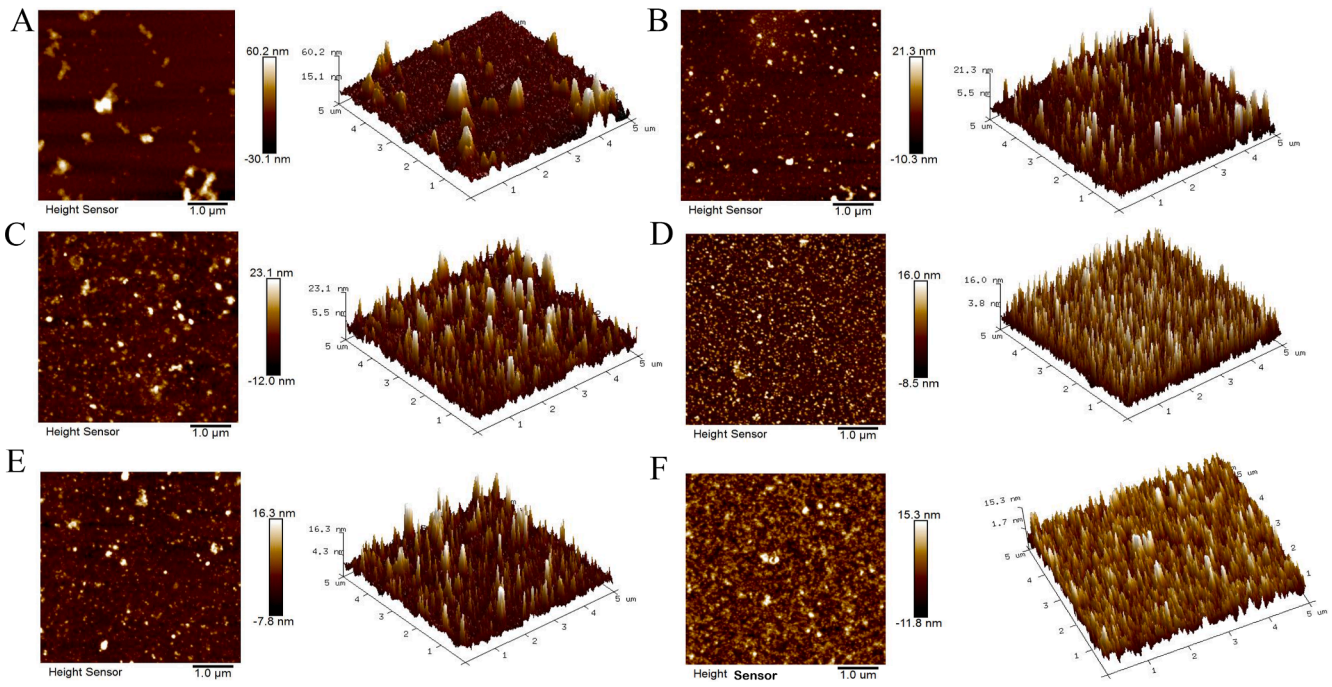

Fig. 3. The AFM of PPI and treated PPI samples. (A: PPI; B: UPPI; C: PPI-10; D: UPPI-10; E: PPI-12; F: UPPI-12).

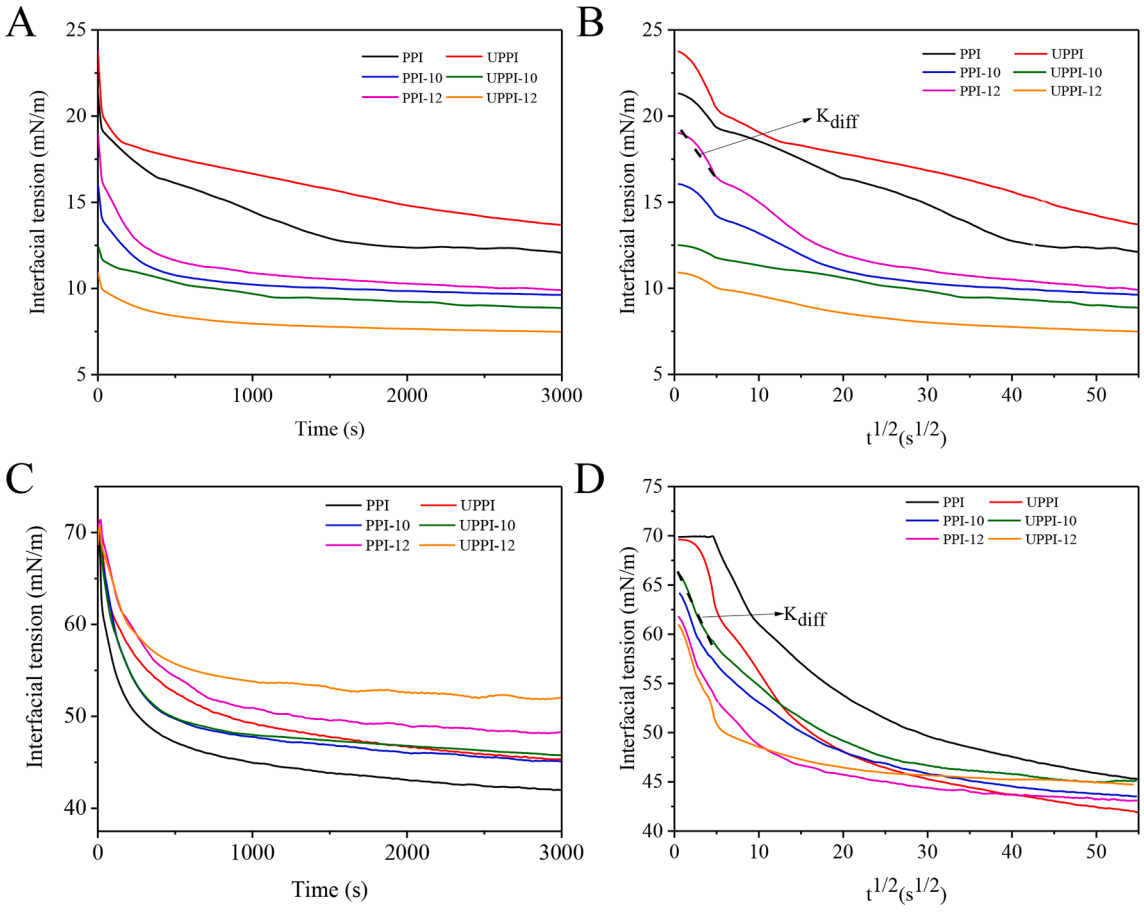

Fig. 4. Time evolution of the interfacial tension (mN/m) for the adsorption of PPI and treated PPI samples at the oil (MCT)-water (A-B) and air -water (C-D) interfaces (K_{diff} quantifies the diffusion rate).

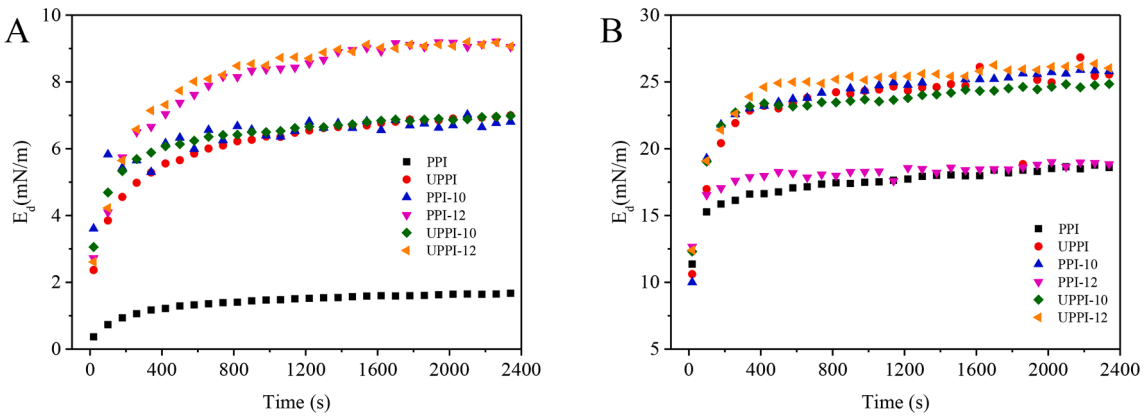

Fig. 5. The interfacial elastic modulus (E_d) of PPI and treated PPI samples at the oil (MCT)/water interface (A) and air/water interface (B).

most likely reason for the faster adsorption rate.

Fig. 5 exhibits the time-dependent changes of the interfacial dilatational rheological properties. In all cases, the interfacial elastic modulus (E_d) of PPI samples was much larger than viscous modulus (E_v, data not shown), indicating that the oil- and air–water interfaces stabilized by PPI samples were dominated by elasticity. This indicated that alkaline treatment and ultrasound treatment alone could significantly improve the elastic modulus of PPI. The effect of ultrasonic-assisted pH shift treatment was significant ($p < 0.05$), indicating that the treatment enhanced the elasticity of the PPI-stabilized interfacial films. For the air–water interface, the E_d of PPI at the investigated end point was 18.59 mN/m, and the UPPI-12 treated with ultrasonic synergy with pH was highest (26.03 mN/m), indicating that ultrasound synergistic pH treatment could significantly improve the elasticity of PPI ($p < 0.05$).

3.3. Cryo-SEM and Confocal-Raman microscopy analysis

In order to reveal the microstructures and assembly behaviors of PPI samples on the oil–water interface, the morphology of the interfacial film was further observed by cryo-SEM (Fig. 6). For the untreated PPI group, the larger spherical-like PPI particles covered on the interface were captured. The voids were obviously seen among the protein particles at the interface, reflecting the relatively loose arrangement on the interface (Fig. 6**A and B**). The size of PPI after ultrasound treatment alone was not much different from the control, but it can be seen that the attached proteins at the interface include large-sized proteins and small-sized proteins (Fig. 6**C and D**). The interfacial adsorbed protein size of PPI was further reduced after pH shift treatment alone (Fig. 6**E and F**). The particle size of UPPI-12 was further obviously reduced. Their arrangement on the interfaces was denser and smoother (Fig. 6**G and H**). This indicated that tight interfacial layers better prevent the coalescence and coarsening of emulsion droplets. UPPI-12 had increased β-sheet and ordered structure, so it might cause the interfacial films with tighter structure [50–53].

In Raman confocal spectroscopy, laser light can be focused on a spot on the sample to obtain Raman spectral information of this spot [54]. Selected regions of PPI adsorbed at the MCT-water interface are shown in **Fig. S1**. The corresponding Raman spectra of the modified PPI-stabilized interfacial layer is shown in Fig. 7. The doublet at 1265 and 1341 cm^{-1} is the amide III band, corresponding to the coupling of C—N stretching and N—H bending motion. The peak at 1662 cm^{-1} is from the amide I band of the protein [55]. Compared with PPI in the bulk solution, an interesting phenomenon was captured, in which PPI adsorbed at the oil–water interface showed obviously weak absorption peak at 1600–1700 cm^{-1}. Besides, a peak around 1744 cm^{-1} was significantly strengthened for all investigated samples except for UPPI-12. This special phenomenon might be due to the remodeling of the PPI at the interface, which resulted in structural changes. This might also be because other components in the protein, such as polyphenols, could migrate to the interface, thus leading to the changes in protein conformation. The specific internal mechanism needs to be further studied.

3.4. Functional properties of PPI

3.4.1. Solubility

The solubility of proteins is considered to be the most practical indicator to measure the functional properties of proteins. An increase in solubility can improve the performance of proteins [41,43]. Therefore, good solubility is a prerequisite for using proteins as emulsifiers and foaming agents. The solubility of different samples is shown in Fig. 8. The solubility of PPI was 48.19 %. After being treated with alkaline, and ultrasonic-assisted pH shift treatment, it was significantly improved ($p < 0.05$). The solubility of PPI-12, UPPI-10, and UPPI-12 increased to 97.37 %, 99.13 %, and 98.90 %, respectively. Mechanical forces, such as shear force generated by cavitation, could destroy the hydrophobic, electrostatic interaction, hydrogen bond, and other non-covalent interactions in the aggregated protein. This caused conformational changes and the formation of soluble protein aggregates from insoluble states [43]. Thus, the protein solubility could be improved. Studies showed that ultrasound treatment increased the solubility of black soybean protein from 47 % to 51 % [44], pea protein from 8 % to 56 % [15], and barley protein from 16 % to 27 % [2]. Moreover, the UPPI-12 not only had a smaller particle size but also possessed the higher solubility. After alkaline shift processing, the structure of PPI unfolded and became more flexible. Now if coupled with ultrasound, the physical forces could alter the microstructure of PPI to a greater extent, thereby obtaining the smaller aggregates and increasing the solubility. Alavi et al. [1] also found that the solubility of faba bean proteins with the combined alkaline shifting and ultrasound drastically increased more than 95 %.

3.4.2. Emulsifying properties

Emulsification characteristics are generally evaluated by EAI and ESI, in which EAI measures the ability of the proteins to be adsorbed at the interface and ESI evaluates the performance of the formed adsorbed layer [56]. As shown in Fig. 9**A and B**, the EAI of natural PPI was the lowest (8.07 m^2/g). The EAI of PPI-10, PPI-12, UPPI-10, and UPPI-12 was increased to 9.11 m^2/g, 9.04 m^2/g, 11.65 m^2/g, and 12.85 m^2/g, respectively. This might be due to their enhanced adsorption rate to the oil–water interface, resulting from the suitable surface hydrophobicity, smaller particle size, and improved solubility. This caused a rapid reduction in the interfacial tension [57]. The ESI of PPI increased significantly after treatment. Meanwhile, some similar observations to improve the emulsification properties of protein by ultrasound treatment, such as wheat gluten, peanut protein isolate, quinoa protein isolate, and other legume protein, were reported [58]. UPPI-12 reached

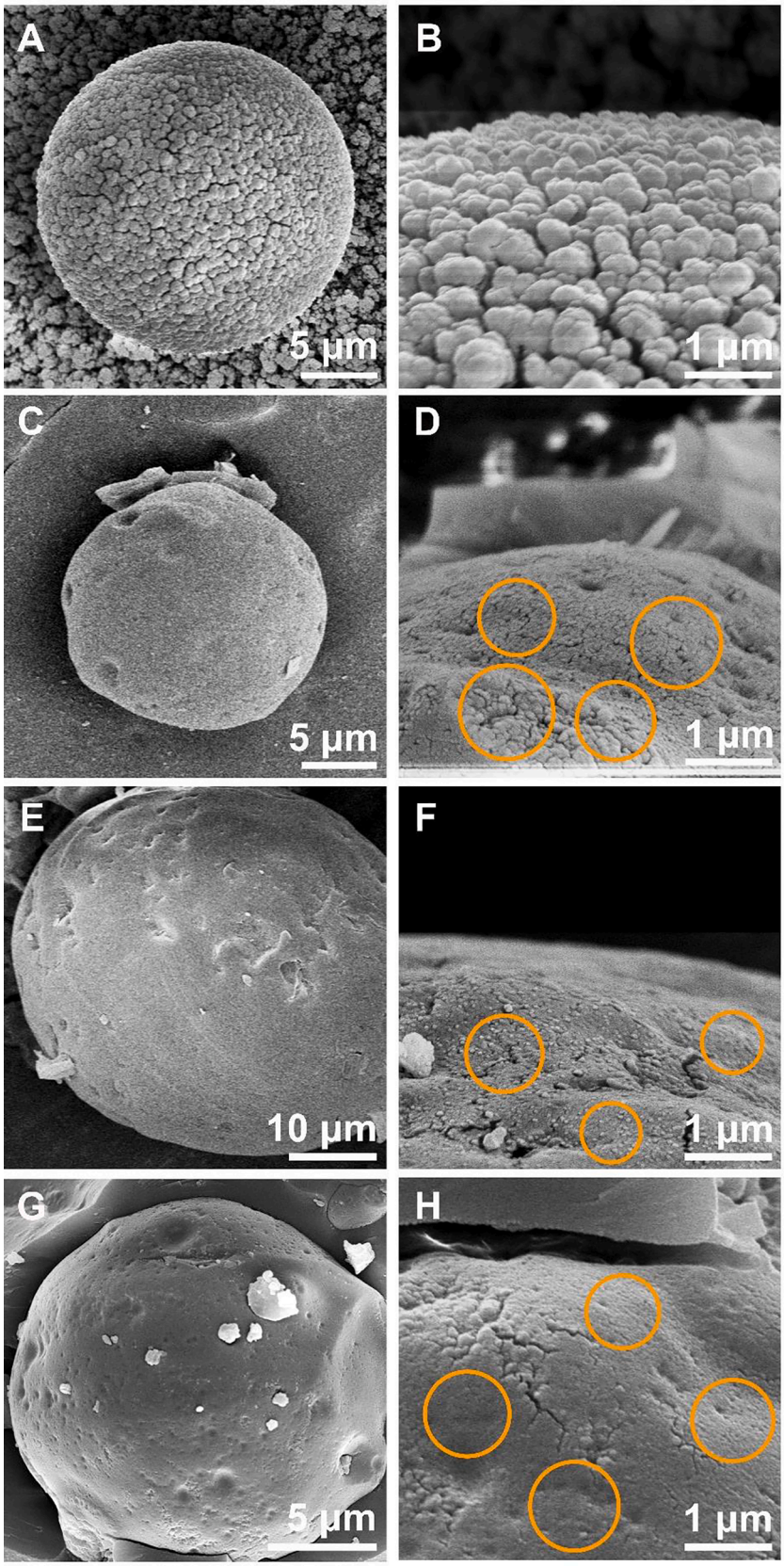

Fig. 6. The cryo-SEM of PPI and treated PPI samples. (A, B: PPI; C, D: UPPI; E, F: PPI-12; G, H: UPPI-12).

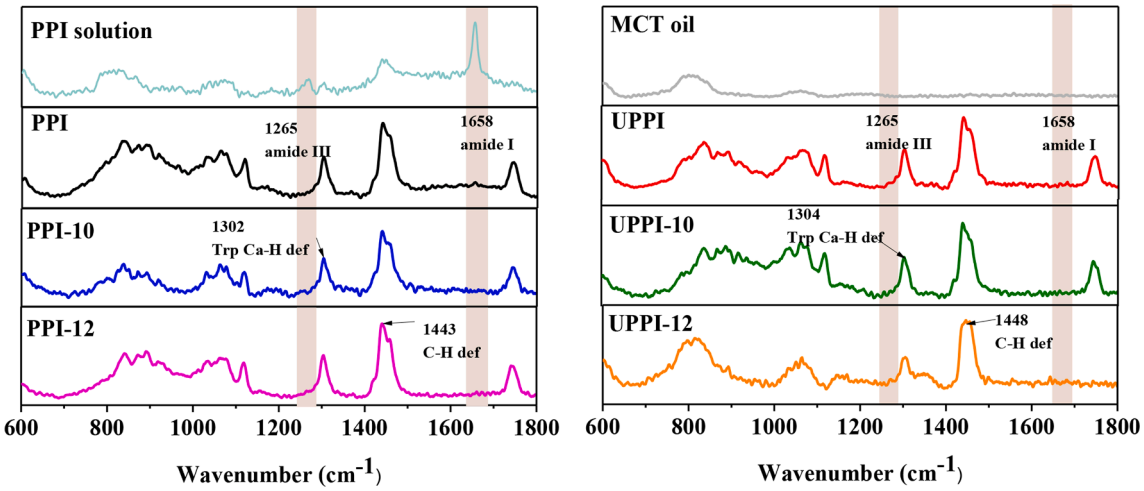

Fig. 7. Confocal-Raman spectra of the oil-water interface stabilized by assembled PPI and treated PPI samples.

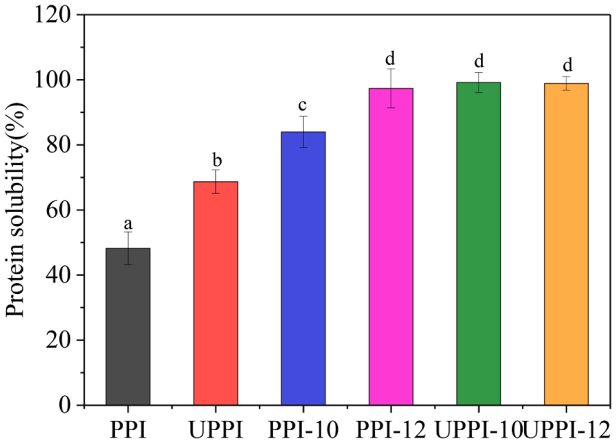

Fig. 8. The solubility of PPI and treated PPI samples.

the maximum ESI value of 79.54 min. This might be due to the flexible structure of protein which resulted in a larger elastic modulus of interfacial film, which slowed down the rate of coalescence and disproportionation of emulsion droplets [41,59]. Amine et al. [60] reported that the interfacial tension had a good correlation with the formation of the emulsion.

3.4.3. *Foaming properties*

The foaming behaviors of the control and treated PPI samples are evaluated, and the results are shown in Fig. 9**C and D**. The foamability of the control was 41 %. Alkali treatment alone (PPI-10 and PPI-12) and ultrasound treatment alone improved the foamability of PPI to 91 % and 135 %, respectively. This resulted from the faster adsorption rate to the air/water interface of proteins treated by alkali or ultrasound [61]. Interestingly, ultrasonic-assisted pH shift treatment could significantly affect the foamability of PPI. UPPI-12 possessed the foamability of 160 %, which was 3.9 times than that of PPI. The higher surface hydrophobicity, smaller particle size, and larger solubility made the UPPI-12 having the fastest adsorption rate, which could reduce the interfacial energy barrier, and thus increase foamability. Ultrasonic-assisted pH shift treatment also could significantly affect the foam stability of PPI. UPPI-12 possessed foam stability of 71.40 %, which was 1.32 times that of PPI. The foam stability of a protein is mainly relevant to the viscoelastic properties of interfacial films formed by protein [62]. The alkali-coupled with ultrasound could increase the elastic modulus of interfacial film, which prevented the drainage, coalescence, and disproportionation of bubbles, thus enhancing the foam stability.

We analyzed the above results and obtained the following speculation. PPI had a slow adsorption rate and formed a loose interfacial structure with weak in-plane interactions, resulting from the larger particle size and lower surface hydrophobicity. When the PPI was treated by ultrasound alone, the β-sheet increased and α-helix decreased. This might induce an increase in surface hydrophobicity. As a result, UPPI could be adsorbed more quickly at the air- and oil–water interfaces and form viscoelastic interfacial films with stronger in-plane interactions. Meanwhile, UPPI-10/12 had the fastest adsorption rate and could form a stiff and compact viscoelastic interfacial structure, thus promoting its emulsifying and foaming properties.

4. Conclusions

The effects of ultrasonic-assisted pH shift treatment on the structure, interfacial behaviors, and functional properties of PPI were determined. The particle size of protein aggregates significantly reduced and the solubility of PPI could reach 99 % after ultrasonic-assisted pH shift treatment. Compared to PPI, UPPI-12 possessed enhanced emulsifying and foaming properties, which might be due to the fast adsorption rate and high elastic modulus at the oil-/ air–water interfaces, resulting from the higher surface hydrophobicity, smaller particle size, changed secondary structure, and improved solubility. In contrast, alkaline shift or ultrasound alone showed less improvement in emulsifying and foaming properties of PPI. After ultrasonic-assisted pH shift treatment, the structure of PPI was unfolded, as well as the β-sheet further increased and α-helix continued to decrease, which endowed the PPI with a smaller size and larger surface hydrophobicity. The present study suggested that ultrasonic-assisted pH shift treatment was a useful means to modify PPI to enhance their functional properties. Besides, the modified PPI still needs to be further explored for the evaluation of nutrition and digestion. Structural identification of modified proteins and *in vivo* and *in vitro* experiments should be the main goals of follow-up studies.

CRediT authorship contribution statement

Jing Yang: Investigation, Formal analysis, Validation, Data curation, Writing – original draft, Visualization. **Fang Geng:** Methodology, Data curation. **Chen Cheng:** Formal analysis. **Lei Wang:** Formal analysis. **Jieting Ye:** Formal analysis. **Haihui Zhang:** Methodology, Data curation. **Dengfeng Peng:** Conceptualization, Funding acquisition, Methodology, Writing – review & editing, Supervision. **Qianchun Deng:** Conceptualization, Methodology, Writing – review & editing, Supervision, Project administration.

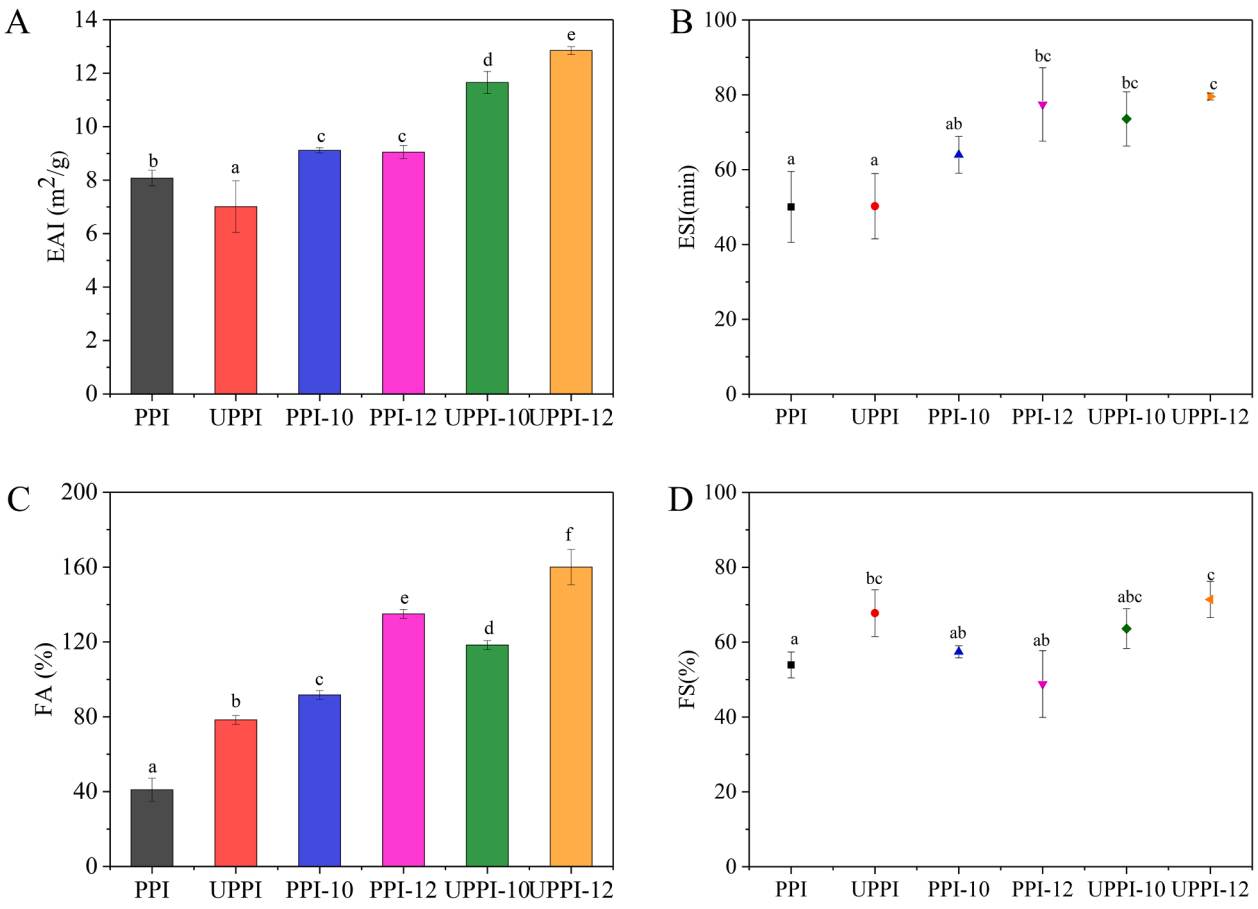

Fig. 9. The (A) emulsifying activity (EAI), (B) emulsifying stability (ESI), (C) foamability (FA), and (D) foaming stability (FS) of PPI and treated PPI samples.

Declaration of Competing Interest

The authors declare that they have no known competing financial interests or personal relationships that could have appeared to influence the work reported in this paper.

Acknowledgements

This research was funded by National Natural Science Foundation of China (32102020), Key Research projects of Hubei Province (2020BCA086), Wuhan Application Fundamental Frontier Project of China (2020020601012270), and National Key Research and Development Program of China (2021YFD2100400). We thank Dr. Cuie Tang of Huazhong Agricultural University for the help in the use of far-UV circular dichroism (CD) spectroscopy.

Appendix A. Supplementary data

Supplementary data to this article can be found online at https://doi.org/10.1016/j.ultsonch.2022.106108.

References

[1] F. Alavi, L. Chen, Z. Emam-Djomeh, Effect of ultrasound-assisted alkaline treatment on functional property modifications of faba bean protein, Food Chem. 354 (2021), 129494.
[2] P. Silventoinen, N. Sozer, Impact of ultrasound treatment and pH-shifting on physicochemical properties of protein-enriched barley fraction and barley protein isolate, Foods 9 (2020) 1055.
[3] Q. Zhao, L. Wang, X. Hong, Y. Liu, J. Li, Structural and functional properties of perilla protein isolate extracted from oilseed residues and its utilization in Pickering emulsions, Food Hydrocolloids 113 (2021), 106412.
[4] Q. Zhao, Q. Gu, X. Hong, Y. Liu, J. Li, Novel protein-based nanoparticles from perilla oilseed residues as sole Pickering stabilizers for high internal phase emulsions, LWT - Food Sci. Technol. 145 (2021), 111340.
[5] N. Liu, Q. Chen, G. Li, Z. Zhu, J. Yi, C. Li, X. Chen, Y. Wang, Properties and stability of Perilla seed protein-stabilized oil-in-water emulsions: influence of protein concentration, pH, NaCl concentration and thermal treatment, Molecules 23 (2018) 1533.
[6] Q. Fan, P. Wang, X. Zheng, S.S. Hamzah, H. Zeng, Y. Zhang, J. Hu, Effect of dynamic high pressure microfluidization on the solubility properties and structure profiles of proteins in water-insoluble fraction of edible bird's nests, LWT 132 (2020), 109923.
[7] C. Wen, J. Zhang, H. Yao, J. Zhou, Y. Duan, H. Zhang, H. Ma, Advances in renewable plant-derived protein source: the structure, physicochemical properties affected by ultrasonication, Ultrason. Sonochem. 53 (2019) 83–98.
[8] Q. Zhao, W. Yan, Y. Liu, J. Li, Modulation of the structural and functional properties of perilla protein isolate from oilseed residues by dynamic high-pressure microfluidization, Food Chem. 365 (2021), 130497.
[9] Q. Zhao, T. Xie, X. Hong, Y. Zhou, L. Fan, Y. Liu, J. Li, Modification of functional properties of perilla protein isolate by high-intensity ultrasonic treatment and the stability of o/w emulsion, Food Chem. 368 (2022) 130848.
[10] Y. Tian, Z. Zhang, P. Zhang, A. Taha, H. Hu, S. Pan, The role of conformational state of pH-shifted β-conglycinin on the oil/water interfacial properties and emulsifying capacities, Food Hydrocolloids 108 (2020), 105990.
[11] J. Jiang, Q. Wang, Y.L. Xiong, A pH shift approach to the improvement of interfacial properties of plant seed proteins, Curr. Opin. Food Sci. 19 (2018) 50–56.
[12] L.J. Deleu, M.A. Lambrecht, J. Van de Vondel, J.A. Delcour, The impact of alkaline conditions on storage proteins of cereals and pseudo-cereals, Curr. Opin. Food Sci. 25 (2019) 98–103.
[13] R. Mercadé-Prieto, S. Gunasekaran, Alkali cold gelation of whey proteins. Part I: Sol−Gel−Sol(−Gel) transitions, Langmuir 25 (10) (2009) 5785–5792.
[14] H. Lee, G. Yildiz, L.C. dos Santos, S. Jiang, J.E. Andrade, N.J. Engeseth, H. Feng, Soy protein nano-aggregates with improved functional properties prepared by sequential pH treatment and ultrasonication, Food Hydrocolloids 55 (2016) 200–209.
[15] S. Jiang, J. Ding, J. Andrade, T.M. Rababah, A. Almajwal, M.M. Abulmeaty, H. Feng, Modifying the physicochemical properties of pea protein by pH-shifting and ultrasound combined treatments, Ultrason. Sonochem. 38 (2017) 835–842.
[16] Y. Li, Y. Cheng, Z. Zhang, Y. Wang, B.K. Mintah, M. Dabbour, H. Jiang, R. He, H. Ma, Modification of rapeseed protein by ultrasound-assisted pH shift treatment:

ultrasonic mode and frequency screening, changes in protein solubility and structural characteristics, Ultrason. Sonochem. 69 (2020), 105240.
[17] L. Zhang, Z. Pan, K. Shen, X. Cai, B. Zheng, S. Miao, Influence of ultrasound-assisted alkali treatment on the structural properties and functionalities of rice protein, J. Cereal Sci. 79 (2018) 204–209.
[18] S. Pezeshk, M. Rezaei, H. Hosseini, M. Abdollahi, Impact of pH-shift processing combined with ultrasonication on structural and functional properties of proteins isolated from rainbow trout by-products, Food Hydrocolloids 118 (2021), 106768.
[19] L.-P. Peng, C.-H. Tang, Outstanding antioxidant pickering high internal phase emulsions by co-assembled polyphenol-soy β-conglycinin nanoparticles, Food Res. Int. 136 (2020), 109509.
[20] X. Shi, H. Zou, S. Sun, Z. Lu, T. Zhang, J. Gao, C. Yu, Application of high-pressure homogenization for improving the physicochemical, functional and rheological properties of myofibrillar protein, Int. J. Biol. Macromol. 138 (2019) 425–432.
[21] N. Walayat, Z. Xiong, H. Xiong, H.M. Moreno, A. Nawaz, N. Niaz, C. Hu, M.I. Taj, B. S. Mushtaq, I. Khalifa, The effect of egg white protein and β-cyclodextrin mixture on structural and functional properties of silver carp myofibrillar proteins during frozen storage, LWT 135 (2021), 109975.
[22] Y. Shen, X. Tang, Y. Li, Drying methods affect physicochemical and functional properties of quinoa protein isolate, Food Chem. 339 (2021), 127823.
[23] T.-K. Kim, H.I. Yong, H.H. Chun, M.-A. Lee, Y.-B. Kim, Y.-S. Choi, Changes of amino acid composition and protein technical functionality of edible insects by extracting steps, J. Asia-Pac. Entomol. 23 (2020) 298–305.
[24] V. García Arteaga, M. Apéstegui Guardia, I. Muranyi, P. Eisner, U. Schweiggert-Weisz, Effect of enzymatic hydrolysis on molecular weight distribution, techno-functional properties and sensory perception of pea protein isolates, Innovative Food Sci. Emerg. Technol. 65 (2020), 102449.
[25] D. Peng, J. Yang, J. Li, C. Tang, B. Li, Foams stabilized by β-lactoglobulin amyloid fibrils: effect of pH, J. Agric. Food. Chem. 65 (48) (2017) 10658–10665.
[26] C. Wen, J. Zhang, H. Zhang, Y. Duan, H. Ma, Effects of divergent ultrasound pretreatment on the structure of watermelon seed protein and the antioxidant activity of its hydrolysates, Food Chem. 299 (2019), 125165.
[27] X. Wang, K. Yu, C. Cheng, D. Peng, X. Yu, H. Chen, Y. Chen, D. Julian McClements, Q. Deng, Effect of sesamol on the physical and chemical stability of plant-based flaxseed oil-in-water emulsions stabilized by proteins or phospholipids, Food Funct. 12 (5) (2021) 2090–2101.
[28] E. Kirtil, T. Svitova, C.J. Radke, M.H. Oztop, S. Sahin, Investigation of surface properties of quince seed extract as a novel polymeric surfactant, Food Hydrocolloids 123 (2022) 107185.
[29] Z.-L. Wan, L.-Y. Wang, J.-M. Wang, Y. Yuan, X.-Q. Yang, Synergistic foaming and surface properties of a weakly interacting mixture of soy glycinin and biosurfactant stevioside, J. Agric. Food. Chem. 62 (2014) 6834–6843.
[30] Y. Guo, C. Wu, M. Du, S. Lin, X. Xu, P. Yu, In-situ dispersion of casein to form nanoparticles for Pickering high internal phase emulsions, LWT 139 (2021), 110538.
[31] F. Jiang, Y. Pan, D. Peng, W. Huang, W. Shen, W. Jin, Q. Huang, Tunable self-assemblies of whey protein isolate fibrils for pickering emulsions structure regulation, Food Hydrocolloids 124 (2022), 107264.
[32] M.M. Bradford, A rapid and sensitive method for the quantitation of microgram quantities of protein utilizing the principle of protein-dye binding, Anal. Biochem. 72 (1976) 248–254.
[33] T.S.P. de Souza, F.F.G. Dias, M.G.B. Koblitz, J.M.L.N. de Moura Bell, Effects of enzymatic extraction of oil and protein from almond cake on the physicochemical and functional properties of protein extracts, Food Bioprod. Process. 122 (2020) 280–290.
[34] D. Peng, W. Jin, L.M.C. Sagis, B. Li, Adsorption of microgel aggregates formed by assembly of gliadin nanoparticles and a β-lactoglobulin fibril-peptide mixture at the air/water interface: Surface morphology and foaming behavior, Food Hydrocolloids 122 (2022), 107039.
[35] W. Xiong, Y. Wang, C. Zhang, J. Wan, B.R. Shah, Y. Pei, B. Zhou, J. Li, B. Li, High intensity ultrasound modified ovalbumin: structure, interface and gelation properties, Ultrason. Sonochem. 31 (2016) 302–309.
[36] H. Zou, N. Zhao, S. Sun, X. Dong, C. Yu, High-intensity ultrasonication treatment improved physicochemical and functional properties of mussel sarcoplasmic proteins and enhanced the stability of oil-in-water emulsion, Colloids Surf. A: Physicochem. Eng. Aspects 589 (2020), 124463.
[37] Q. Cui, L. Wang, G. Wang, A. Zhang, X. Wang, L. Jiang, Ultrasonication effects on physicochemical and emulsifying properties of Cyperus esculentus seed (tiger nut) proteins, LWT 142 (2021), 110979.
[38] H. Zhang, G. Chen, M. Liu, X. Mei, Q. Yu, J. Kan, Effects of multi-frequency ultrasound on physicochemical properties, structural characteristics of gluten protein and the quality of noodle, Ultrason. Sonochem. 67 (2020), 105135.
[39] F. Wang, Y. Zhang, L. Xu, H. Ma, An efficient ultrasound-assisted extraction method of pea protein and its effect on protein functional properties and biological activities, LWT 127 (2020), 109348.
[40] C. Mao, J. Wu, X. Zhang, F. Ma, C. Yu, Improving the solubility and digestibility of potato protein with an online ultrasound-assisted PH shifting treatment at medium temperature, Foods 9 (2020) 1908.
[41] L. Chen, J. Chen, J. Ren, M. Zhao, Effects of ultrasound pretreatment on the enzymatic hydrolysis of soy protein isolates and on the emulsifying properties of hydrolysates, J. Agric. Food. Chem. 59 (2011) 2600–2609.
[42] J. Chandrapala, B. Zisu, M. Palmer, S. Kentish, M. Ashokkumar, Effects of ultrasound on the thermal and structural characteristics of proteins in reconstituted whey protein concentrate, Ultrason. Sonochem. 18 (2011) 951–957.
[43] H. Hu, J. Wu, E.C.Y. Li-Chan, L. Zhu, F. Zhang, X. Xu, G. Fan, L. Wang, X. Huang, S. Pan, Effects of ultrasound on structural and physical properties of soy protein isolate (SPI) dispersions, Food Hydrocolloids 30 (2013) 647–655.
[44] J. Jiang, B. Zhu, Y. Liu, Y.L. Xiong, Correction to interfacial structural role of pH-shifting processed pea protein in the oxidative stability of oil/water emulsions, J. Agric. Food Chem. 62 (2014) 4225.
[45] J. Weiss, K. Kristbergsson, G. Kjartansson, Engineering Food Ingredients with High-Intensity Ultrasound, Ultrasound Technol. Food Bioprocessing (2011) 239–285.
[46] J. O'Sullivan, B. Murray, C. Flynn, I. Norton, The effect of ultrasound treatment on the structural, physical and emulsifying properties of animal and vegetable proteins, Food Hydrocolloids 53 (2016) 141–154.
[47] Q. Ding, T. Zhang, S. Niu, F. Cao, R.A. Wu-Chen, L. Luo, H. Ma, Impact of ultrasound pretreatment on hydrolysate and digestion products of grape seed protein, Ultrason. Sonochem. 42 (2018) 704–713.
[48] D. Peng, W. Jin, M. Arts, J. Yang, B. Li, L.M.C. Sagis, Effect of CMC degree of substitution and gliadin/CMC ratio on surface rheology and foaming behavior of gliadin/CMC nanoparticles, Food Hydrocolloids 107 (2020), 105955.
[49] D. Peng, W. Jin, J. Li, W. Xiong, Y. Pei, Y. Wang, Y. Li, B. Li, Adsorption and distribution of edible gliadin nanoparticles at the air/water interface, J. Agric. Food. Chem. 65 (2017) 2454–2460.
[50] S. Cohen-Addad, R. Höhler, Rheology of foams and highly concentrated emulsions, Curr. Opin. Colloid Interface Sci. 19 (2014) 536–548.
[51] E. Dickinson, Structure formation in casein-based gels, foams, and emulsions, Colloids Surf., A 288 (1-3) (2006) 3–11.
[52] Y.-T. Xu, C.-H. Tang, T.-X. Liu, R. Liu, Ovalbumin as an outstanding pickering nano-stabilizer for high internal phase emulsions, J. Agric. Food. Chem. 66 (33) (2018) 8795–8804.
[53] O.S. Deshmukh, D. van den Ende, M.C. Stuart, F. Mugele, M.H.G. Duits, Hard and soft colloids at fluid interfaces: adsorption, interactions, assembly & rheology, Adv. Colloid Interface Sci. 222 (2015) 215–227.
[54] Z. Wei, J. Cheng, Q. Huang, Food-grade Pickering emulsions stabilized by ovotransferrin fibrils, Food Hydrocolloids 94 (2019) 592–602.
[55] K. Wang, D.-W. Sun, Q. Wei, H. Pu, Quantification and visualization of α-tocopherol in oil-in-water emulsion based delivery systems by Raman microspectroscopy, LWT 96 (2018) 66–74.
[56] M.A. Malik, H.K. Sharma, C.S. Saini, High intensity ultrasound treatment of protein isolate extracted from dephenolized sunflower meal: effect on physicochemical and functional properties, Ultrason. Sonochem. 39 (2017) 511–519.
[57] I. Suppavorasatit, E. Mejia, K. Cadwallader, Optimization of the enzymatic deamidation of soy protein by protein-glutaminase and its effect on the functional properties of the protein, J. Agric. Food. Chem. 59 (2011) 11621–11628.
[58] M. Hadidi, A. Ibarz, S. Pouramin, Optimization of extraction and deamidation of edible protein from evening primrose (Oenothera biennis L.) oil processing by-products and its effect on structural and techno-functional properties, Food Chem. 334 (2021), 127613.
[59] M.H. Kamani, J. Semwal, M.S. Meera, Functional modification of protein extracted from black gram by-product: effect of ultrasonication and micronization techniques, LWT 144 (2021), 111193.
[60] C. Amine, J. Dreher, T. Helgason, T. Tadros, Investigation of emulsifying properties and emulsion stability of plant and milk proteins using interfacial tension and interfacial elasticity, Food Hydrocolloids 39 (2014) 180–186.
[61] J. Yang, G. Liu, H. Zeng, L. Chen, Effects of high pressure homogenization on faba bean protein aggregation in relation to solubility and interfacial properties, Food Hydrocolloids 83 (2018) 275–286.
[62] P. Wierenga, M. Meinders, M. Egmond, A. Voragen, Protein exposed hydrophobicity reduces the kinetic barrier for adsorption of ovalbumin to the air-water interface, Langmuir 19 (2003) 8964–8970.